

# A steady trickle-down from metro districts and improving epidemic-parameters characterized the increasing COVID-19 cases in India

Santosh Ansumali<sup>a,d</sup>, Alope Kumar<sup>b</sup>, Samarth Agarwal<sup>a</sup>, H. J. Shashank<sup>a</sup>,  
Meher K. Prakash<sup>1c,e</sup>

<sup>a</sup>*Engineering Mechanics Unit, Jawaharlal Nehru Centre for Advanced Scientific Research, Jakkur, Bangalore, India*

<sup>b</sup>*Department of Mechanical Engineering, Indian Institute of Science, Bangalore, India*

<sup>c</sup>*Theoretical Sciences Unit, Jawaharlal Nehru Centre for Advanced Scientific Research, Jakkur, Bangalore, India*

<sup>d</sup>*Sankhya Sutra Labs, Manyata Embassy Business Park, Bengaluru, Karnataka, India*

<sup>e</sup>*VNIR Biotechnologies Pvt Ltd, Bangalore Bioinnovation Center, Helix Biotech Park, Electronic City Phase I, Bangalore, India*

---

## Abstract

**Background** By mid-September of 2020, the number of daily new infections in India crossed 95,000. We aimed to characterize the spatio-temporal shifts in the disease burden as the infections rose during the first wave of COVID-19.

**Methods** We gathered the publicly available district-level (equivalent of counties) granular data for the 15 April to 31 August 2020 period. We used the epidemiological data from 186 districts with the highest case burden as of August 31, 559,566 active cases and 2,715,656 cumulative infections, and the governing epidemic parameters were estimated by fitting it to a susceptible-asymptomatic-infected-recovered-dead (SAIRD) model. The space-time trends in the case burden and epidemic parameters were analyzed. When the physical proximity of the districts did not explain the spreading patterns, we developed a metric for accessibility of the districts via air and train travel. The districts were categorized as large metro, metro, urban and sub-urban and the spatial shifts in

---

<sup>1</sup>Corresponding Author: [meher@jncastr.ac.in](mailto:meher@jncastr.ac.in)

case burden were analyzed.

**Results** The center of the burden of the current-active infections which on May 15 was in the large metro districts with easy international access shifted continuously and smoothly towards districts which could be accessed by domestic airports and by trains. A linear trend-analysis showed a continuous improvement in the governing epidemic parameters consistently across the four categories of districts. The reproduction numbers improved from  $1.77 \pm 0.58$  on May 15 to  $1.07 \pm 0.13$  on August 31 in large metro districts (p-Value of trend 0.0001053); and from  $1.58 \pm 0.39$  on May 15 to  $0.94 \pm 0.11$  on August 31 in sub-urban districts (p-Value of trend 0.0067). The recovery rate per infected person per day improved from  $0.0581 \pm 0.009$  on May 15 to  $0.091 \pm 0.010$  on August 31 in large metro districts (p-Value of trend  $0.26 \times 10^{-12}$ ); and from  $0.059 \pm 0.011$  on May 15 to  $0.100 \pm 0.010$  on August 31 in sub-urban districts (p-Value of trend  $0.12 \times 10^{-16}$ ). The death rate of symptomatic individuals which includes the case-fatality-rate as well as the time from symptoms to death, consistently decreased from  $0.0025 \pm 0.0014$  on May 15 to  $0.0013 \pm 0.0003$  on August 31 in large metro districts (p-Value of trend 0.0010); and from  $0.0018 \pm 0.0008$  on May 15 to  $0.0014 \pm 0.0003$  on August 31 in sub-urban districts (p-Value of trend 0.2789).

**Conclusions** As the daily infections continued to rise at a national level, the “center” of the pandemic-burden shifted smoothly and predictably towards smaller sized districts in a clear hierarchical fashion of accessibility from an international travel perspective. This observed trend was meant to serve as an alert to re-organize healthcare resources towards remote districts. The geographical spreading patterns continue to be relevant as the second wave of infections began in March 2021 with a center in the mid-range districts.

**Funding** None

*Keywords:* Case-burden, Epidemic diffusion, Hotspots, granular, Time-varying epidemic-parameters, Reproduction ratio, COVID-19, India

---

## 1 Introduction

2 In the COVID-19 pandemic that began in December 2019, each month  
3 witnessed the critical rise of infections in completely different countries. The  
4 initial declaration of national emergency which was a "one-size fits all" was  
5 quickly irrelevant in many countries as each state or county perceived the  
6 need for stringency differently. The differences arose mainly because even  
7 within the first wave of the pandemic, the solidarity extended through inter-  
8 state loans of ventilators demonstrated how at any given time the geograph-  
9 ical regions in different phases of the pandemic, rising, stable or declining,  
10 perceived the threat differently from others. As the rise of infections in dif-  
11 ferent geographical regions is asynchronous, the critical care burden shifts  
12 dynamically with each region attempting to achieve its 'local-flattening' of  
13 the peak at a different time. The focus shifted towards regional containment  
14 COVID-19 containment strategies, for which identifying the next hotspots  
15 became extremely important[1, 2].

16 Epidemiological models have focused on making predictions of the rise of  
17 infections, and a peak of critical care burden on a country or a state basis.  
18 There have been longitudinal studies[3, 4] demonstrating how the reproduc-  
19 tion number varied over time in the different states or countries and possibly  
20 correlating it to the effects of lockdowns. Further, a few cross-sectional stud-  
21 ies correlated the hotspots in the spread of infections in the initial phase to  
22 the traffic flow out of Wuhan.[5] These studies mostly focused on one region  
23 at a time, either on estimating parameters, or making projections. In this  
24 work, we build a summarizing perspective of the geographical development  
25 of the pandemic, by analyzing a cumulative 2.71 million infections and 52  
26 thousand deaths of COVID-19 from India over a period of four and a half  
27 months.

28 To examine how the hotspots of COVID-19 spread over time across India,  
29 we identified the districts of interest based on case-burden, estimated the  
30 time-varying epidemiological parameters for these regions, categorized these  
31 regions according to the ease of travel access in the hierarchical order of  
32 availability of international flights, domestic flights, trains or other quater-  
33 nary modes of transport, and analyzed the trends in parameters over time in  
34 each of these categories. The data shows predictable shifts to remote regions.  
35 The infections spreading to newer and under-catered locations presents both  
36 an opportunity and a challenge, an asynchronous peak of critical require-

37 ments which can be addressed both by manufacturing and re-organizing the  
38 resources on an *ad hoc* basis.

39

## Research in context

### Evidence before this study

We searched *pubmed* and *medRxiv* up to 20 September 2020 with the keywords “COVID-19”, “time variation or longitudinal”, “cantons or states”, “hotspots”, “diffusion” “active-cases”. The published research thus far focused mainly on reporting either the time variation of reproduction number at the state-level, or the predictions of rise of infections at the canton level. However, from these constantly updating predictions with new hotspots appearing, there is no continuity of knowledge and possibility to obtain a comprehensive picture of the development of the pandemic. A study correlating the number of infections in different regions in China to the traffic-flow out of Wuhan, and another describing the development of hotspots along the highways in Brazil describe some aspects of this geographical spread. Firstly, a similar analysis with granular Indian data has been missing. Further, the questions of how the center of the active-case burden diffused and the spatio-temporal trends in epidemiological parameters underlying the large number of infections have not been the focus of these earlier studies.

### Added value of this study

Our study begins with the understanding that the different geographic regions such as districts (or counties) may be in different phases of the pandemic, and the mixing of population within a district is more likely than across the different districts. Considering this geographical heterogeneity, and the ease of access to these different districts, we develop a summary of how the pandemic evolved in the regions of different accessibility over a period of four-and-a-half months. Predictable trends in the case-burden diffusion are identified.

### Implications of all the available evidence

Authorities should understand the shift in the dynamics of the critical-care requirements, not by geographically contiguous regions, but by ease of travel or by common economic interests which guided such ease of travel. Strategies should be driven by knowing where the pandemic burden is likely to move, before it happens. The trend of the case-burden predictably shifting towards suburban districts can  
40 be useful in re-organizing the available resources as per the needs.

## 41 **Methods**

### 42 *COVID-19 Data*

43 The district-wise COVID-19 daily new infections, daily active cases and daily  
44 deaths were gathered from a publicly available data repository:  
45 <http://www.covid19india.org>. The age, sex demographics of the infected peo-  
46 ple in these districts were not available. Using a criterion of at least 20 daily  
47 new infections on 31 August 2020, 186 districts were identified and used in  
48 the analysis. These 186 districts accounted for 2,715,656 of the 3,687,939  
49 cumulative infections in India, and had an active case burden of 559,566  
50 from the 785,127 total active infections in India. These 186 districts out  
51 of the 739 districts in India, account for a 696 million population in 2020,  
52 estimated from the 2001 and 2011 census data. The data spans across 22 dif-  
53 ferent states which are currently governed by many different political parties,  
54 which is likely to reduce any inherent and centralized biases in the data.

### 55 *Model*

56 An important feature of COVID-19 is the role played by asymptomatics in  
57 the spread of the disease.[6] Classic compartmental models such as the sus-  
58 ceptible infected-recovered (SIR) models fail to account for this important  
59 aspect of the disease and thus one should work with models where asymp-  
60 tomatic fraction is explicitly included in the model. In this work, we extended  
61 the susceptible-asymptomatic-infected-recovered (SAIR) model we developed  
62 earlier[7] by including the deaths (D), and used this SAIRD model to estimate  
63 the underlying epidemic parameters for each district. The compartmental na-  
64 ture of the model is shown schematically in Figure (1A) and the governing  
65 equations are given in Figure (1B). The asymptomatics in this framework are  
66 assumed to include the pre-symptomatics who subsequently become symp-  
67 tomatic as well as those who will continue to remain asymptomatic until  
68 their recovery. The rates of recovery and transmission of infections of the  
69 asymptomatic and the symptomatic individuals are assumed to be the same.  
70 The model thus relies on four different epidemiological parameters - infection  
71 rate ( $\beta$ ), recovery rate ( $\gamma$ ), death rate ( $\gamma_D$ ), asymptomatic to symptomatic  
72 conversion ( $\delta$ ), which we extracted from the data as follows.

### 73 *Parameter Estimation*

74 Even in the simplest scenario of the exponential growth with of infections  
75  $I$  with time, we found that choosing a linear fit between  $dI/dt$  and  $I$  led

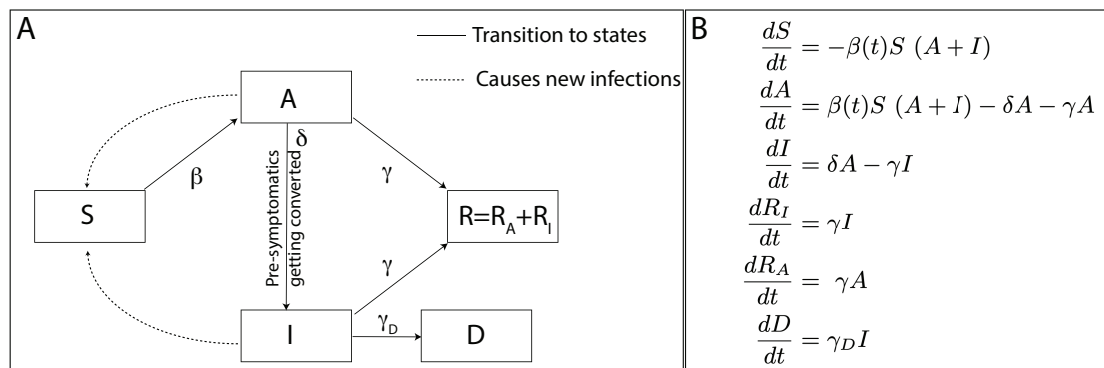


Figure 1: *A.* A schematic of the SAIRD model and its *B.* modelling equations used in the present analysis. The SAIR model on which this scheme is based is described in Ref. [7]. The parameters used in these equations are assumed to be constant over different segments of the pandemic trajectory (piece-wise continuous) and were estimated by fitting the predictions for infections, recoveries, and deaths over time.

76 to a better parameter estimation than an exponential fit between  $I$  and  $t$ ,  
 77 although both are mathematically equivalent.[8] The parameter estimation  
 78 scheme we evolved[7] for all the parameters thus relies on rearranging the un-  
 79 derlying equations in a way that allowed us to provide most reliable estimates  
 80 despite the uncertainties and noise in the data. The time-varying epidemi-  
 81 ological parameters were estimated for the different districts. The infection  
 82 spread-rate ( $\beta$ ), recovery-rate ( $\gamma$ ) and the death-rate ( $\gamma_D$ ) were estimated in  
 83 a time-dependent way, identifying time periods over which a single parameter  
 84 best describes the observations. The (pre- or) asymptomatic to symptomatic  
 85 conversion rate ( $\delta$ ) was assumed to be a constant for each district.

86  $\gamma(t)$  **estimation.** To estimate  $\gamma$  we note that,  $dR_I/dt = \gamma I$ , which can be  
 87 easily integrated to obtain  $R_I(t_2) - R_I(t_1) = \gamma \left( \int_{t_1}^{t_2} I dt \right)$ . However, it is  
 88 well understood that  $\gamma$  changes over time owing to changes in policies and  
 89 behavioral patterns. We note that the plot for  $R_I$  vs.  $\int I dt$  is piecewise linear  
 90 and the value of  $\gamma$  for different periods can be calculated using simple linear  
 91 regression and estimating the slope.

92  $\gamma_D(t)$  **estimation.** The estimation for  $\gamma_D$  then follows in a similar procedure.  
 93  $dD/dt = \gamma_D I$ , which is integrated to obtain  $D(t_2) - D(t_1) = \gamma_D \left( \int_{t_1}^{t_2} I dt \right)$ .

94  $\beta(t)$  **estimation.** To estimate  $\beta$  we employ  $\log I(t) \sim (\beta - \gamma) t$ .

95  $\delta$  **estimation.** The values of the hidden asymptomatics and  $\delta$  are determined

96 using a grid search and then choosing the values which provide the best fit.  
97 The estimates of  $\delta$  for the 186 districts were  $0.34 \pm 0.02$ , which corresponds  
98 to a timescale of  $4.23 \pm 0.48$  days. This timescale is comparable to the mean  
99 incubation time estimates [9].

100  **$R_t$  estimation.** The time-dependent reproduction ratio,  $R_t$ , which is an  
101 effective measure of the current status of the spread of the infection and its  
102 containment was obtained from the ratio  $\beta(t)/\gamma(t)$ .

103

#### 104 *Linear trend analysis*

105 The various epidemic parameters we estimated were analysed for the presence  
106 of a significant trend. This linear trend analysis was performed using the  
107 Matlab module `regstats` and the significance values were obtained using  
108 `stats.tstat.pval`.

#### 109 *Travel accessibility of districts*

110 The ease of travel-access to the districts was defined using the *pre-pandemic*  
111 airplane and train connectivity. The international and domestic flight traf-  
112 fic to the different airports was gathered from the Airports Authority of India  
113 website (<https://www.aai.aero/sites/default/files/traffic-news/Mar2k20Annex2.pdf>),  
114 and it was assigned to the respective districts. The train station with the  
115 highest through-traffic in each district was noted using the data from the  
116 *ClearTrip* travel website (<https://www.cleartrip.com/trains/stations/list>). A  
117 combined metric for travel accessibility was developed where the districts  
118 were ranked 1 to 8 and further grouped into four categories - *Large metro*  
119 *districts*: International airports with an *annual* traffic of more than 25,000  
120 flights (1), more than 5,000 flights (2), with any direct international flights  
121 (3), *Metro districts*: more than 5000 *annual* domestic flights (4), any domes-  
122 tic flights (5), *Urban districts*: more than 50 trains stopping in the district  
123 (6), more than 20 trains (7), and *Sub-urban districts*: all districts with other  
124 quaternary means of reaching (8).

## 125 **Results**

### 126 *Hotspots are not contiguous*

127 During the April 15-August 31 of 2021, the number of COVID-19 infec-  
128 tions in India rose continuously from around 1,000 daily new infections to

129 around 80,000 daily new infections. The initial epicenters were in the large  
130 metropolitan cities such as New Delhi (from the state of Delhi) and Mumbai  
131 (from the state of Maharashtra). With lockdowns and non-pharmaceutical  
132 interventions, the case burden in these cities reduced, but there was a com-  
133 comitant rise of COVID-19 cases in many smaller districts. The active-case  
134 burden diffused out of large metro districts. However, mapping the hotspot  
135 districts in the geographic map of the India certainly does not immediately  
136 reveal how the infections increased or spread. An example of the develop-  
137 ment of hotspots in the state of Maharashtra is shown in Figure 2. One  
138 may immediately notice two exceptions - that newer hotspot districts need  
139 not be contiguous with the existing hotspots and further some of the con-  
140 tiguous districts did not develop into hotspots. Thus it is apparent that a  
141 plain spatial diffusion model is not sufficient to address the hotspots that  
142 appear non-contiguously. We needed an alternative framework to interpret  
143 the development of the hotspots.

#### 144 *Correlating hotspots with international travel accessibility*

145 Since COVID-19 infections started with import of cases, we asked if the down-  
146 stream development of newer hotspots is also related to the ease of accessing  
147 a district from an international perspective by various means of transport.  
148 We ranked the districts 1 to 8 depending upon the level of accessibility, and  
149 further categorized the districts as large metro, metro, urban and sub-urban  
150 districts using a hierarchical accessibility by international airports, domestic  
151 airports, train hubs and other quaternary means of transport, respectively  
152 (**Methods**). In Figure 3, we show the number of active COVID-19 cases  
153 during the period May 15 - August 31 across the districts in four broad ac-  
154 cessibility categories. The figure clarifies that the hotspots in each state,  
155 represented by a sector, spread radially outwards suggesting a spread away  
156 from the districts with international airports towards districts which are only  
157 accessible only via trains. The states where the most accessible regions have  
158 not yet recorded a lot of infections, did not also a downstream spread of in-  
159 fections into their remote districts. The figure highlights the significant role  
160 of importation of the cases, and a weak or poor-mixing across different states  
161 initially due to lockdowns, followed by quarantines upon inter-state travels  
162 during phased release of the lockdown.



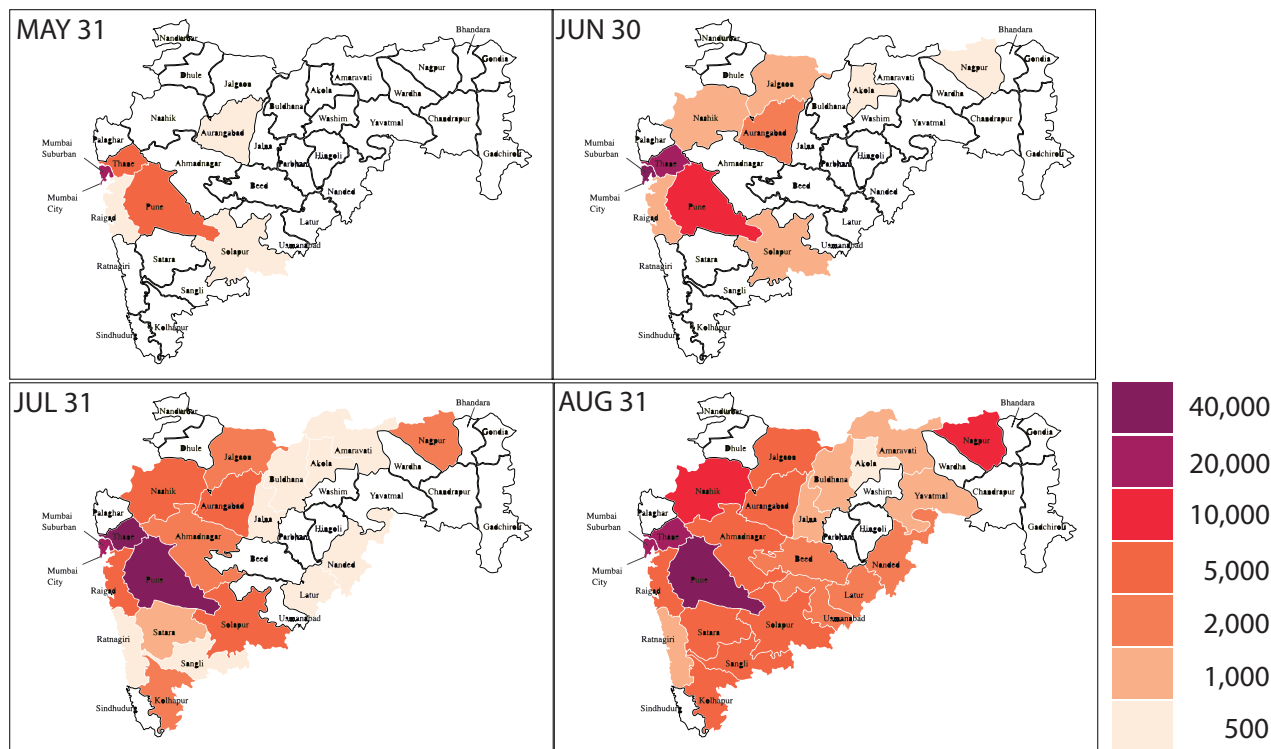


Figure 2: Evolution in time of the pandemic over the districts as seen in the geographic map of Maharashtra. The active case burden is approximated to the nearest cluster indicated in the color-bar. One can see that the the spread of the infections is at times continuous, and on some other occasions begins in districts disconnected from the current hotspots.

163 *The pandemic-burden shifted away from larger metros in the first wave*  
 164 As the infections continued to grow in numbers as well as spread across  
 165 the country, it is important to know where the current center of the dis-  
 166 ease burden is, and if there is a predictable shift in its position. We de-  
 167 fined the current center of active case burden by weighing the number of  
 168 currently active cases with the accessibility level (1 to 8) of the district  
 169 as  $(\sum_{districts} I_{district} \times accessibility) / (\sum_{districts} I_{district})$ . The result shown in  
 170 Figure 4 suggests a continuous and smooth drift of this center of active cases  
 171 away from the large metro districts towards least accessible districts. The  
 172 districts which are not easily accessible, are also usually the ones with lesser  
 173 health care resources. The result underscores the need for planning and de-  
 174 ploying resources towards regions which do not have adequate testing and  
 175 critical health care support.

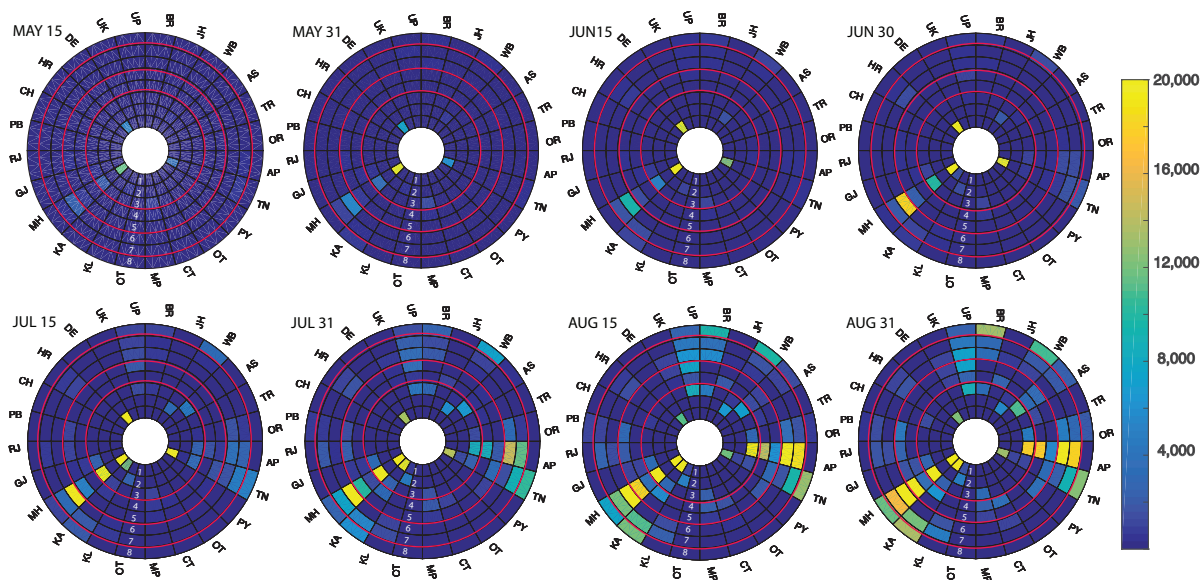


Figure 3: Evolution in time of the pandemic over the districts. Each sector represents the state denoted by its 2 letter code, such as DE for Delhi, MH for Maharashtra. The 8 different layers from inside to outside are the ones in the decreasing order of accessibility. These 8 layers are further clustered as those having international airports, having only domestic airports, connected only by trains and have no train or airplane connections, and are separated by the red-circles. In each state, the hotspots continue to move outwards as the time progresses. Two segments labeled OT are meant other states, which are not included in the analysis.

176 The peak of the first wave of infections was reached in mid-September 2020,  
177 and the number of infections in the various regions we studied decreased  
178 without any further geographical spread. In mid March 2021, the alarm  
179 about the second wave of infections began as over 40,000 daily new cases  
180 were reported. The epidemiological data from this early stages of the second  
181 wave shows an interesting pattern that the districts with the highest number  
182 of infections are mainly with medium or low accessibility (Figure 4). As the  
183 second wave progresses, these patterns need to be reassessed to understand  
184 or validate the role of mobility across the districts.

185 *Infections continued to rise, but with lower Reproduction numbers.*

186 In addition to this geographical spread, we also analyzed the temporal trends  
187 in the epidemic parameters from the different regions. During the rising  
188 phase of the first wave of infections even as the number of newly reported

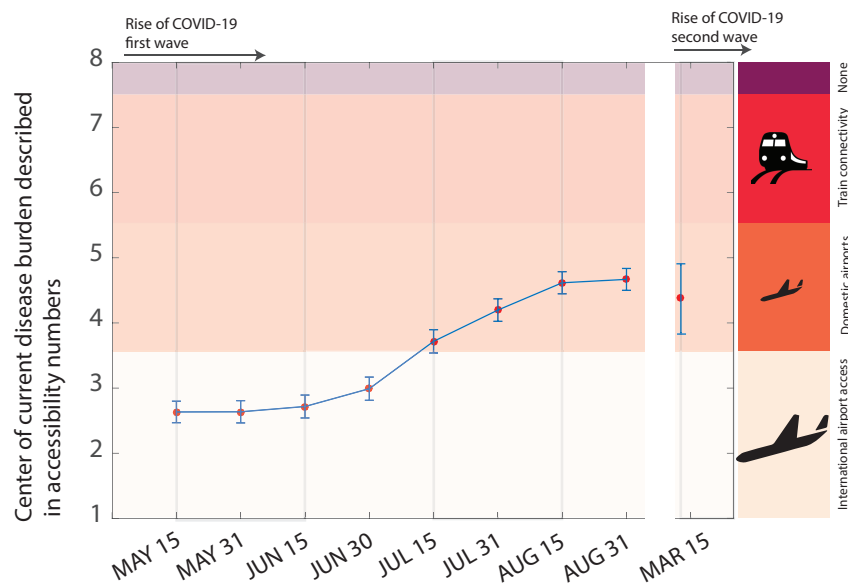


Figure 4: The current burden of the active cases is calculated by weighing the active cases in each district by its accessibility code (1-internationally accessible large metro; 8-least accessible district, as indicated in Figure 3). One can see a clear shift of the case burden away from the large cities. The accessibility of the districts through international, domestic airports and trains are indicated. Also shown is the infection burden as of March 15, 2021 at the beginning of the second wave of COVID-19 infections, which in a way seems to continue with the spread of infections in small and hard to access districts.

189 cases and currently active cases continued to rise (Figure 5A), one can notice  
 190 from the slopes that the rate of infection rise continues to decrease in  
 191 districts of all levels of accessibility. The time varying reproduction number  
 192 ( $R_t$ ) estimates from our analysis over the May 15-August 31 period which  
 193 witnessed phased release of lockdowns suggest values which are much less  
 194 than the basic reproduction number estimates between 2.5 to 4. The average  
 195 reproduction number across the districts of different accessibility showed a de-  
 196 creasing trend (Figure 5B). A linear trend analysis suggested the large metro  
 197 and sub-urban districts have a reduction in  $R_t$  with p-Values of 0.0001053  
 198 and 0.0067 respectively. While the average reproduction numbers appear  
 199 to reduce even in metro and urban districts, the trends were not significant  
 200 (p-Values of 0.4634 and 0.4618 respectively).

201 In order to distinguish if the slow down of infections occurred because of a  
 202 herd immunity or because of the changes in behavioural patterns, we exam-

203 ined the infected percentage (=cumulative infections/population  $\times$  100%)  
204 of the population at which the  $R_t$  dropped below one. The infected per-  
205 centages vary significantly, for example in the two contiguous districts of  
206 Mumbai and Pune, these values were 0.25% symptomatic and 1.08% includ-  
207 ing asymptomatics in Mumbai and 0.7% symptomatic and 2.21% including  
208 asymptomatics in Pune, which suggests that the slowdown of infections is  
209 achieved because of changes in behavioural patterns and an exercise of cau-  
210 tion was still required to maintain the pandemic in control.

211 The trends in the reproduction numbers in the second wave of the COVID-19  
212 infections need to be examined when the sufficient number of infections are  
213 built over time to yield reliable predictions of the epidemic parameters across  
214 the different districts. Further, any such analyses will also need to account  
215 for the presence role of different mutants.

#### 216 *Recovery and death rates improved*

217 The time to recovery from the time of appearance of symptoms for the symp-  
218 tomatic patients ( $1/\gamma$ ) estimated for the 186 districts as  $16.18 \pm 1.01$  on May  
219 15 was consistent with the 24.7 (22.9-28.1) that was reported in the early  
220 days of infections from China.[10]. However, by August 31, the recovery  
221 time showed an improvement as ( $\gamma$ ) decreased to  $10.08 \pm 0.69$  on August  
222 31. The time variation of recovery rates ( $\gamma$ ) is shown in Figure 5C, and  
223 the trend analysis suggested an increase in the recovery rates with p-values  
224  $0.2667 \times 10^{-12}$ ,  $0.5504 \times 10^{-3}$ ,  $0.9180 \times 10^{-37}$ ,  $0.1250 \times 10^{-16}$  in the large metro,  
225 metro, urban and sub-urban districts. Similarly death rates  $\gamma_D$  which is a  
226 product of the case fatality rate (reported as  $\approx 2\%$  in India, and consistent  
227 with an  $\approx 10$  days time to death) with the rate of death also showed an  
228 improvement over the time with p-Values of 0.0010, 0.0122,  $0.6272 \times 10^{-3}$ ,  
229 0.2789 respectively in the large metro, metro, urban and sub-urban districts  
230 (Figure 5D).

#### 231 *Comparison with other studies*

232 In an analysis of the spread of SARS across countries,[11] it was realized  
233 that a smooth spatial diffusion of pandemic which was sufficient to describe  
234 Black Death[12] could not address a quicker reach of the epidemic to many  
235 cities. It was demonstrated that the time taken for the epidemic arrival  
236 time to the different cities was correlated not to the geographic distance  
237 from the epicenter, but rather to an effective distance defined by the degree

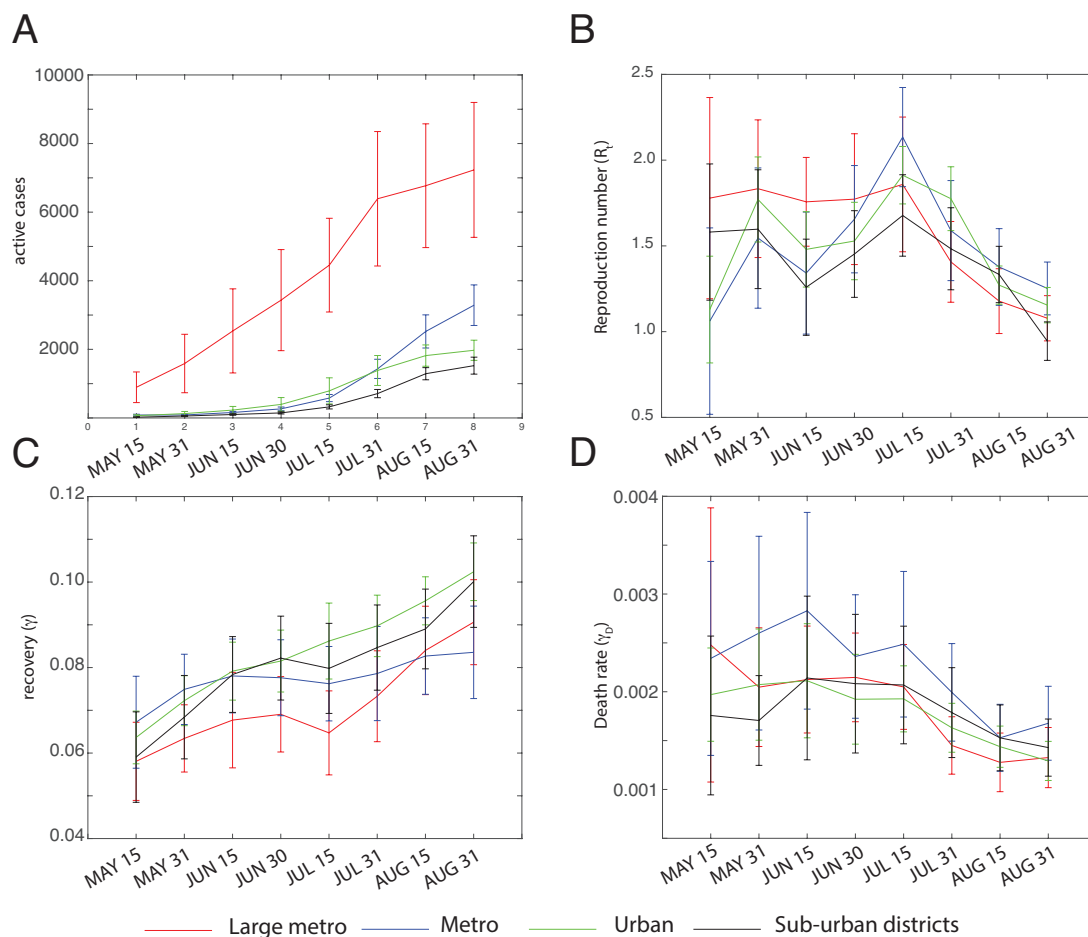


Figure 5: The trends in different epidemiological parameters *A*. Number of daily new infections, *B*. Reproduction number, *C*. Recovery rate ( $\gamma$ ) *D*. Death-rate ( $\gamma_D$ ) are shown for the districts categorized by their accessibility is shown. The trends across the different districts groups are consistent. The reproduction rates, recovery and death rates are all improving, despite the increase in the new infections.

238 of connectivity between the different international airports. The work thus  
239 introduced the concepts of development of epidemics that go beyond simple  
240 spatial diffusion.[12] In a cross-sectional analysis, the development of case-  
241 load of the infections in the different hotspots in China was correlated to  
242 the outflow of traffic from Wuhan in the period January 1 to January 24.[5]  
243 In another recent study on COVID-19 in Brazil, the connectivity between  
244 different cities via highways was attributed to be one of the reasons for super-  
245 spreading across major cities.[13] However, the work did not establish any  
246 patterns for the spread of the active-case burden or its flattening,[14] which  
247 is extremely important in an epidemic or a pandemic from the public health  
248 point-of-view.

249 While the present work is in line with all three works noted above in term  
250 of travel connectivity, there are several unique aspects we discovered in our  
251 study of the COVID-19 data from India. The global spread of pandemic  
252 from Wuhan to different major international destinations may have followed  
253 the similar pattern of effective-distance.[11] However, the emphasis, from the  
254 perspective of incidence within a country and critical resource planning is on  
255 the granular data within the country. Further, unlike the travel outflow which  
256 was obtained by tracking mobiles,[5] the accessibility we use via airplane and  
257 train-connectivity data from *pre*-pandemic period is believed to be a surro-  
258 gate for the degree of connectivity and mixing among the populations. In  
259 the *network science* parlance, this is an emphasis on the centrality-measures  
260 which define the relative importance of the different cities that are being  
261 connected, by-passing the actual connectivity data which is harder to ob-  
262 tain, especially because our study was not limited to a single phase such as  
263 the January 1 to January 24.[5] Finally, by developing the hierarchical ac-  
264 cessibility network, we could show trends such as the radial spreading out  
265 towards remote areas in each state and a smooth variation of the current-  
266 case-burden in Figure 4. Figures 3 and 4, in our opinion go beyond the  
267 immediate requirements of how the infections are rising in a specific region  
268 and serve to provide a wholistic perspective on the development of the pan-  
269 demic as well to help planning for allocating or re-organizing critical care or  
270 test resources towards less catered cities.

## 271 Conclusions

272 In summary, we show predictable trends of improvement of disease parame-  
273 ters, and spread of COVID-19 infection burden away from easily accessible

274 metros with large international airports. The continuing number of cases,  
275 and the predictable drift suggests the need for planning or even reorganizing  
276 testing and critical health care resources to districts which are down-stream  
277 in international access. A lack of correlation between the slow-down of in-  
278 fections and the extent of current infections suggests that the caution and  
279 change in behavioral patterns need to continue if COVID-19 has to be kept  
280 in check.

## 281 **Declarations**

### 282 *Acknowledgements*

283 We acknowledge discussions with Prof. P. Sunthar. MKP and SA acknowl-  
284 edge Aman Sharma and Fauzia Javed for help in gathering the airport and  
285 train traffic data.

### 286 *Availability of data and materials*

287 The analysis was based on publicly available district-wise infection and death  
288 rate available from: <https://www.covid19india.org/>. The district-wise COVID-  
289 19 infection, recovery rates we estimated, the flight and train traffic through  
290 these districts, and the Matlab script used for analysis are all available at:  
291 <https://github.com/meherpr/COVIDIndianDistricts>.

### 292 *Authors' contributions*

293 SAnsumali and MKP conceived and designed the study; SAgrawal performed  
294 the SAIRD model analysis; HJS collected district accessibility data; SAn-  
295 sumali, AK and MKP analyzed the results; SAnsumali and MKP wrote the  
296 manuscript.

### 297 *Ethics approval and consent to participate*

298 The work is an analysis of publicly available epidemiological data. So no  
299 ethics approval is not applicable.

### 300 *Consent for publication*

301 Not applicable.

### 302 *Competing interests*

303 The authors declare that they have no conflicts of interest.

304 *Funding*

305 No funding was received for this research.

306 **References**

- 307 [1] J. Cohen, Scientists are racing to model the next moves of a coronavirus  
308 that’s still hard to predict, *Science* 7 (2020).
- 309 [2] J. Budd, B. S. Miller, E. M. Manning, V. Lampos, M. Zhuang, M. Edel-  
310 stein, G. Rees, V. C. Emery, M. M. Stevens, N. Keegan, et al., Digital  
311 technologies in the public-health response to covid-19, *Nature medicine*  
312 (2020) 1–10.
- 313 [3] S. Flaxman, S. Mishra, A. Gandy, H. J. T. Unwin, T. A. Mellan, H. Cou-  
314 pland, C. Whittaker, H. Zhu, T. Berah, J. W. Eaton, et al., Estimating  
315 the effects of non-pharmaceutical interventions on covid-19 in europe,  
316 *Nature* 584 (2020) 257–261.
- 317 [4] M. Chinazzi, J. T. Davis, M. Ajelli, C. Gioannini, M. Litvinova, S. Mer-  
318 ler, A. P. y Piontti, K. Mu, L. Rossi, K. Sun, et al., The effect of travel  
319 restrictions on the spread of the 2019 novel coronavirus (covid-19) out-  
320 break, *Science* 368 (2020) 395–400.
- 321 [5] J. S. Jia, X. Lu, Y. Yuan, G. Xu, J. Jia, N. A. Christakis, Population  
322 flow drives spatio-temporal distribution of covid-19 in china, *Nature*  
323 (2020) 1–5.
- 324 [6] R. Li, S. Pei, B. Chen, Y. Song, T. Zhang, W. Yang, J. Shaman, Sub-  
325 stantial undocumented infection facilitates the rapid dissemination of  
326 novel coronavirus (sars-cov2), *Science* (2020).
- 327 [7] S. Kaushal, A. S. Rajput, S. Bhattacharya, M. Vidyasagar, A. Kumar,  
328 M. K. Prakash, S. Ansumali, Estimating hidden asymptomatics, herd  
329 immunity threshold and lockdown effects using a covid-19 specific model,  
330 arXiv preprint arXiv:2006.00045 (2020).
- 331 [8] M. K. Prakash, S. Kaushal, S. Bhattacharya, A. Chandran, A. Kumar,  
332 S. Ansumali, Minimal and adaptive numerical strategy for critical re-  
333 source planning in a pandemic, *Physical Review E* 102 (2020) 021301.



- 334 [9] S. A. Lauer, K. H. Grantz, Q. Bi, F. K. Jones, Q. Zheng, H. R. Meredith,  
335 A. S. Azman, N. G. Reich, J. Lessler, The incubation period of coro-  
336 navirus disease 2019 (covid-19) from publicly reported confirmed cases:  
337 estimation and application, *Annals of internal medicine* 172 (2020) 577–  
338 582.
- 339 [10] R. Verity, L. C. Okell, I. Dorigatti, P. Winskill, C. Whittaker, N. Imai,  
340 G. Cuomo-Dannenburg, H. Thompson, P. G. Walker, H. Fu, et al., Es-  
341 timates of the severity of coronavirus disease 2019: a model-based anal-  
342 ysis, *The Lancet infectious diseases* (2020).
- 343 [11] D. Brockmann, D. Helbing, The hidden geometry of complex, network-  
344 driven contagion phenomena, *science* 342 (2013) 1337–1342.
- 345 [12] J. V. Noble, Geographic and temporal development of plagues, *Nature*  
346 250 (1974) 726–729.
- 347 [13] M. A. L. Nicolelis, R. L. G. Raimundo, P. S. Peixoto, C. S. de An-  
348 dreazzi, How super-spreader cities, highways, hospital bed availability,  
349 and dengue fever influenced the covid-19 epidemic in brazil, *medRxiv*  
350 (2020).
- 351 [14] R. M. Anderson, H. Heesterbeek, D. Klinkenberg, T. D. Hollingsworth,  
352 How will country-based mitigation measures influence the course of the  
353 covid-19 epidemic?, *The Lancet* 395 (2020) 931–934.